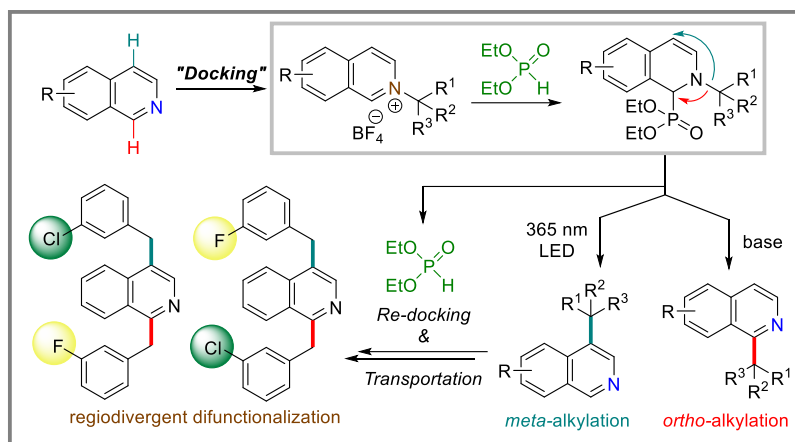


Docking on Azaarene Nitrogen for Phosphite Mediated Sequential Transportations: Switch to *meta*-C–H Alkylation of Isoquinolines

Soniya Rani,^{a,b,†} Anuj Kumar Ray,^{c,‡} Devendra Kumar Dewangan,^{a,b,‡} Nita Aruna Ramchandra Patil,^a Aarthika M,^{a,b} Ankan Paul,^{c,*} and Pradip Maity^{a,b,*}

^aOrganic Chemistry Division, CSIR-National Chemical Laboratory, Pune-411008, India. ^bAcademy of Scientific and Innovative Research (AcSIR), Ghaziabad- 201002, India. ^cSchool of Chemical Sciences, Indian Association for the Cultivation of Science, Kolkata 700032, India.

ABSTRACT: Direct *meta*-C–H alkylation of azaarenes largely remains an unsolved challenge and typically requires multi-step synthesis protocols to circumvent the inherent *ortho/para*-reactivity. Recent progress for direct *meta*-C–H functionalization has been reported, but alkylation remains elusive due to the low reactivity of alkyl halides compared to the other successful electrophiles. We developed a new approach to “dock” the alkyl groups on isoquinoline nitrogen for their phosphite-mediated migrations to C2 carbon for an overall *ortho*-C–H alkylation with complete recovery of the phosphite. Tuning the phosphite-mediated protocol to switch the site selectivity would expedite direct and diverse multi-C–H bond functionalization. Herein, we report a switch to *meta*-C–H alkylation via developing photochemical [1,3] migration of the alkyl group followed by rearomatization. This docking strategy for dual nitrogen activation and C–H functionalization led to a net-zero carbon waste method. The docking and migration protocol works with primary, secondary, and all carbon tertiary alkyl halides, leading to unprecedented success with sterically demanding alkylations. The phosphite-mediated transportation of the alkyl group from nitrogen to ring carbon makes the nitrogen of the *meta*-alkylated isoquinoline product ready for dock again. Here, for the first time, we showed consecutive re-docking of different functional groups on the free isoquinoline nitrogen for their sequential regioselective migrations at *ortho*-position. The change in phosphite-mediated methods and the docking order led to derivatizations of the *meta*-alkylated isoquinoline products, including regiodivergent multi-C–H alkylations of isoquinolines.



INTRODUCTION

Azaarenes with alkyl substitution at different positions are important synthetic goals owing to their frequent occurrence in pharmaceuticals, agrochemicals, chiral ligands, catalysts, and materials.¹ Direct C–H alkylation of abundant and inexpensive azaarenes is the most attractive approach for sustainable and waste-free synthesis.² Among them, isoquinoline core is present in one of the largest numbers of bioactive natural products.³ Substitution at each carbon of the isoquinoline core is prevalent, including *meta*-functionalized bioactive compounds with substituted alkyl groups.⁴ Among different C–H bonds, *ortho*- and *para*-alkylation were achieved successfully with a broad range of electronically and sterically diverse substituents.⁵ However, the *meta*-C–H alkylation remained a formidable challenge due to its inertness towards both electrophilic and nucleophilic rea-

gents. As a result, most of the isoquinoline natural products containing *meta*-alkyl substitution were synthesized from their alkyl substituted acyclic precursors.⁶

In a more direct approach, Minter and Re in 1988 showed a one-pot multi-step operation for effective *meta*-C–H alkylation of isoquinolines with aldehydes (Figure 1A).^{7a} This strategy is based on reductive hydroboration, followed by electrophilic functionalization of the resulting enamine, and finally, dehydration-tautomerization for the overall *meta*-alkylation. The reaction was shown to work only with aldehydes, limiting it to the installation of primary alkyl groups.

In 2022, the Wang group developed an improved Lewis acid catalyzed reductive hydroboration to enamine and its electrophilic functionalization at *meta*-C–H. The catalyst activation led to successful reaction with activated ketones and imines,

along with aldehydes. Additionally, a second equivalent of electrophile oxidized the C3 functionalized enamine intermediate for an overall *meta*-C–H amino and hydroxyl alkylations (Figure 1B).^{7b} In 2023, the Wang group followed up with an asymmetric *meta*-allylation with reactive chiral iridium and palladium π -allyl electrophile.^{7c,d} In 2022, the Kuninobu group utilized a similar approach with silane as the reductant for *meta*-selective trifluoromethylation.^{7e} In these redox approaches, both pre-reduction and post-oxidation steps require extra catalysts and stoichiometric reagents, leading to waste generation. More importantly, activated electrophiles were required for successful *meta*-functionalization, and no reaction was reported with simple alkyl electrophiles such as alkyl halides.

In 2022, Studer and co-workers reported a *meta*-selective radical fluoroalkylation of azaarenes via a redox neutral reaction sequence.^{7f} In 2023, the Donohoe group developed an excess benzoic acid-mediated one-pot *meta*-alkylation of isoquinolines with unsubstituted vinyl ketones, leading to primary alkyl group installation.^{7g} These elegant methods avoid the reduction and oxidation of azaarenes for their *meta*-C–H alkylation. However, they are limited to strong alkylating electrophiles only, owing to a similarly reactive enamine intermediate developed via reduction.^{7a-e} The requirement of stoichiometric reagents to form dearomatized adducts and their removal after alkylation led to waste generation (Figure 1C). A direct and waste-free *meta*-C–H alkylation with unactivated and sterically demanding alkyl halides remains elusive.

One of our research programs focuses on docking functional groups on pyridine nitrogen for their phosphite-catalyzed migrations to the ring carbons (Figure 1D). The “docked” allyl and alkyl groups were successfully migrated to the C2 position for overall *ortho*-allylation and alkylation.⁸ A switch in site selectivity to regiodivergent C–H alkylation from the same N-alkyl pyridinium salts under tunable reaction conditions would be highly advantageous for diversity-oriented synthesis. Regiodivergent switch between *ortho*- and *para*- has been achieved due to their similar electrophilic reactivity pattern. The switch is usually accomplished by taking advantage of the nitrogen coordination to either direct the nucleophile to the *ortho*-position, or sterically block the *ortho*-position with bulky nitrogen-coordinating additives.⁹ However, switching the same functional group between *ortho*-/*para*- and *meta*-C–H bonds is very challenging due to their differential reactivity. Transition metal catalyzed *ortho*-/*para*- and *meta*-C–H activation followed by borylation, arylation, and alkenylations of azaarenes were established recently. The switch in selectivity was achieved via different catalysts with precisely designed ligands.¹⁰ A more attractive electrochemical carboxylation was recently reported by Yu, Lin, and co-workers, where the switch from *meta*- to *para*-carboxylation was achieved simply by using either divided or undivided cells.¹¹ In 2023, the Studer group reported an elegant switch to *para*-C–H alkylation from their previous *meta*-C–H fluoroalkylation via a simple change in pH of the reaction. However, *para*-alkylation needs a nucleophilic alkyl radical coupling partner, while *meta*-fluoroalkylation works with electronically opposite electrophilic radicals.¹² To the best of our knowledge, a switch between *ortho*- and *meta*- by electronically similar alkyl groups has not been reported.

Herein, we report that direct photochemical irradiation at 365 nm LED to the phosphite adduct (2) of N-alkyl docked isoquinolinium (1) resulted in *meta*-C–H alkylation. The unique feature of our approach is the dual role of the docking group to act

as a nitrogen activator to facilitate phosphite adduct (2) formation, followed by its migration from nitrogen to ring carbon. The migration from nitrogen deactivates it, which triggers the in-situ phosphite elimination for an overall C–H functionalization. The recovery and reuse of phosphite after work-up make the overall transformation net-zero in carbon waste. The one-pot method starts with either bench-stable N-alkylisoquinolinium salt 1 or directly from isoquinoline and alkyl halide. Experimental and computational evidence was presented for a plausible mechanism for this unprecedented *meta*-C–H alkylation with primary, secondary, and tertiary alkyl groups. Furthermore, consecutive docking and transportation under the same phosphite-mediated tunable reaction conditions allow for selective and regioisomeric *ortho*, *meta*-di-C–H functionalization with chemically equivalent alkyl halides. The utility of phosphite-mediated methods via nitrogen docking was further demonstrated for the derivatization of *meta*-alkylated products.

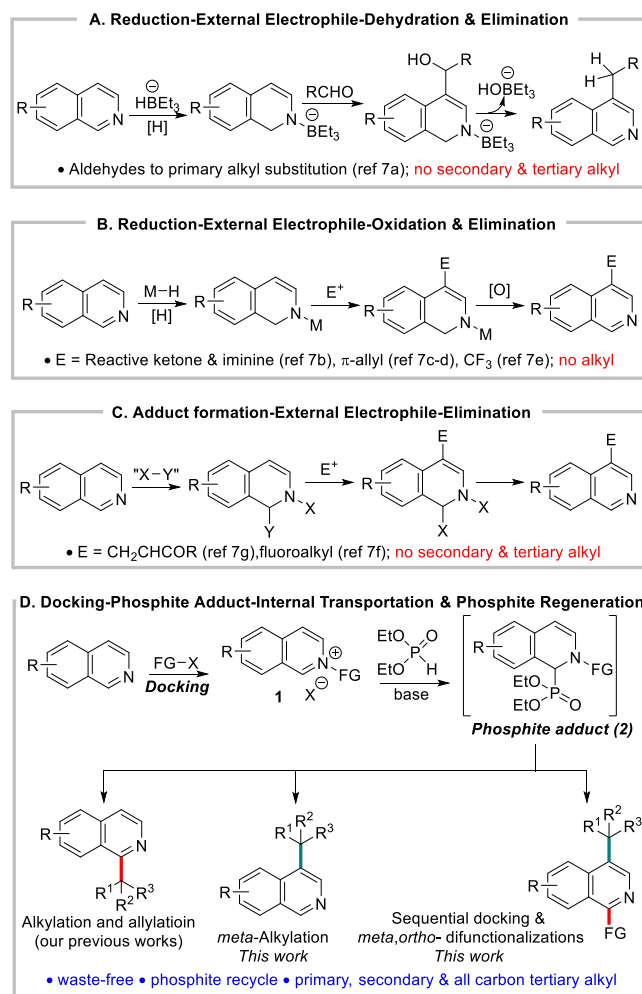


Figure 1. *meta*-C–H alkylations of isoquinolines.

RESULTS AND DISCUSSION

“Docking” of Alkyl groups on Isoquinoline Nitrogen.

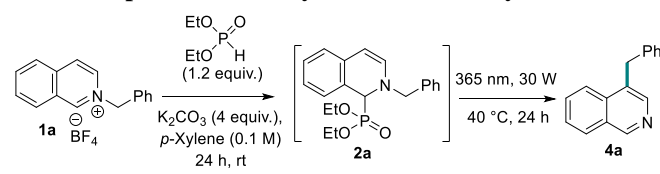
First, we screened conditions for a direct “docking” of alkyl groups on isoquinoline nitrogen. A simple solvent-free mixing of isoquinoline with primary, secondary, and tertiary alkyl halides at ambient to moderate temperature led to the corresponding N-alkyl isoquinolinium halide salt formation with good to excellent yields.¹³ Some of the halide salts are hygroscopic in

nature and form color impurities when stored for months. Literature-modified ion exchange methods were employed to the corresponding tetrafluoroborate salts that are not hygroscopic and are bench stable for years without degradation. A direct tetrafluoroborate salt formation was also achieved via stirring isoquinolines and corresponding alkyl halide in acetone with six equivalents of sodium tetrafluoroborate as an additive.¹⁴

Development of Phosphite mediated photochemical *meta*-Alkylation. We envisioned that the phosphite-adduct **2** of N-isoquinolinium salt could be perceived as an N-alkylated aryl-conjugated enamine or amine-conjugated styrene derivative. The [1,3] O-to-C rearrangement of an O-alkylated aryl-conjugated enol is well-established via both ionic and radical pathways.¹⁵ The corresponding *aza*-version with N-to-C migration is rare, with only one thermal migration known to occur from 1,4-dialkyl-1,4-dihydropyrazines via stereoinversion.¹⁶ We plan to explore a similar N-to-C [1,3] alkyl shift, owing to our previous success with other phosphite-mediated *aza*-migrations around azaarenes.⁸ Thermally heating the phosphite adduct **2** did not result in any migration product.

Next, we explored the possibility of photochemically exciting the amine-conjugated styrene part of the adduct **2** for a possible photochemical *aza*-[1,3] migration. Our photophysical studies of adduct **2** showed that it could be excited with 365 nm light. A fluorescence emission study with excitations at different wavelengths established better absorption at 365 nm with the highest fluorescent emission (see SI). Therefore, we explored a one-pot phosphite addition, followed by its direct excitation for *aza*-[1,3] shift and subsequent base-mediated phosphite elimination for the *meta*-alkylation of isoquinoline (Table 1). Delightfully, the one-pot reaction sequence with stoichiometric phosphite additive in *p*-xylene with four equivalents of potassium carbonate as base led to the *meta*-benzyl isoquinoline in 60% yield with complete regioselectivity (entry 1). Starting with docking to N-benzyl bromide and its one-pot transportation also yielded the product with comparable efficiency (entry 2). Catalytic amounts of phosphite resulted in lower yield with no trace of unreacted starting material or intermediate (**2a**) in the crude reaction mass (entry 3). On the other hand, phosphite was regenerated quantitatively. Therefore, we chose to proceed with stoichiometric phosphite to complete **2a** formation under dark, followed by its photochemical *meta*-alkylation. Diethylphosphite can be separated from the product and other impurities via a simple aqueous work-up protocol (see SI). Reaction in other solvents also formed the product, but the *p*-xylene remains the best (entry 4, see SI for details). Changing base equivalents or other bases led to lower yields (entries 5-7). As anticipated from our photophysical studies, different light sources with higher and lower frequencies led to a drop in reaction efficiencies (entries 8-10). The light intensity is important, with low power light (18W) leads to lower yield (entry 11). No *meta*-benzyl isoquinoline formation was observed without light, and trace amount of product formation was observed without base (entries 12-13).

Table 1. Optimization study of *meta*-C–H Alkylation



Entry ^a	deviation from standard conditions ^a	yield ^b (%)
1	none	60
2 ^c	One-pot with 1a -bromide	58
3	50 mol% phosphite	35
4	Other solvents	5-44
5	3 equiv. of K ₂ CO ₃	54
6	5 equiv. of K ₂ CO ₃	60
7	Other bases	10-50
8	$\lambda_{\text{max}} = 320 \text{ nm}$	<5
9	$\lambda_{\text{max}} = 380 \text{ nm}$	40
10	$\lambda_{\text{max}} = 395 \text{ nm}$	29
11	$\lambda_{\text{max}} = 365 \text{ nm}, 18\text{W}$	34
12	no light	n.d.
13 ^d	no base	<5

^a0.2 mmol scale. ^bisolated yield. n.d. – not detected. ^cone-pot docking and *meta*-alkylation. ^dfor second step

Substrate scope

Under the optimized reaction condition, we screened the substrate scope, focusing on the migrating alkyl group first. A chloro substituent on *ortho*-, *meta*-, and *para*- to the phenyl ring (**4b,c,d**) worked better than the unsubstituted benzyl migrating group. These results indicate that the steric crowd is tolerant around the aryl ring. Other halides at the *meta*-position were equally efficient (**4e,f,g**). The compatibility of all halides at different positions of the aryl substituents is significant since a transition metal catalyzed *meta*-alkylation could be problematic for these substituents. Both electron-deficient groups such as cyano (**4h**) and ester (**4i**), and electron donating methyl (**4j**) and methoxy (**4k**) were well tolerated at the *meta*-position. However, electronically different groups on *para*-position of the phenyl ring drastically affect the reaction outcome. Mildly electron-donating methyl group led to a low 24% yield (**4l**), while strong electron-donating methoxy substitution (**4m**) led to almost no product formation. On the other hand, electron-deficient cyano substitution in *para*-position led to better yield (**4n**). Overall, the electron-neutral and electron-deficient aryl rings resulted in good yields, while electron-rich phenyl groups led to lower efficiencies. With this trend, we tested other non-phenyl aryl groups on migrating benzyl carbon. An electron neutral β -naphthyl (**4o**) and electron-deficient 3- and 4-pyridines gave products (**4p,q**) with good yields, while electron-rich furan (**4r**) and thiophene rings (**4s**) led to lower yields. The better efficiencies with electron-poor group migrations prompt us to try a non-aryl ester substitution on migrating alkyl carbon (**1t**). As anticipated, docking methylene ester group on isoquinoline nitrogen led to the corresponding *meta*-alkylated product (**4t**) in 58% yield. Methyl and *tert*-butyl groups on nitrogen did not form any *meta*-alkylated product. While the N-methyl adduct (**2u**) was unreactive under the optimized reaction condition, the N-*tert*-butyl adduct (**2v**) was completely consumed with only a dimer of *tert*-butyl detected. The scope of our method with substitution on isoquinolines was examined next. We tested a few electron-rich isoquinolines as substrates due to their prevalence in natural products. Methoxy or dimethoxy substitutions on the

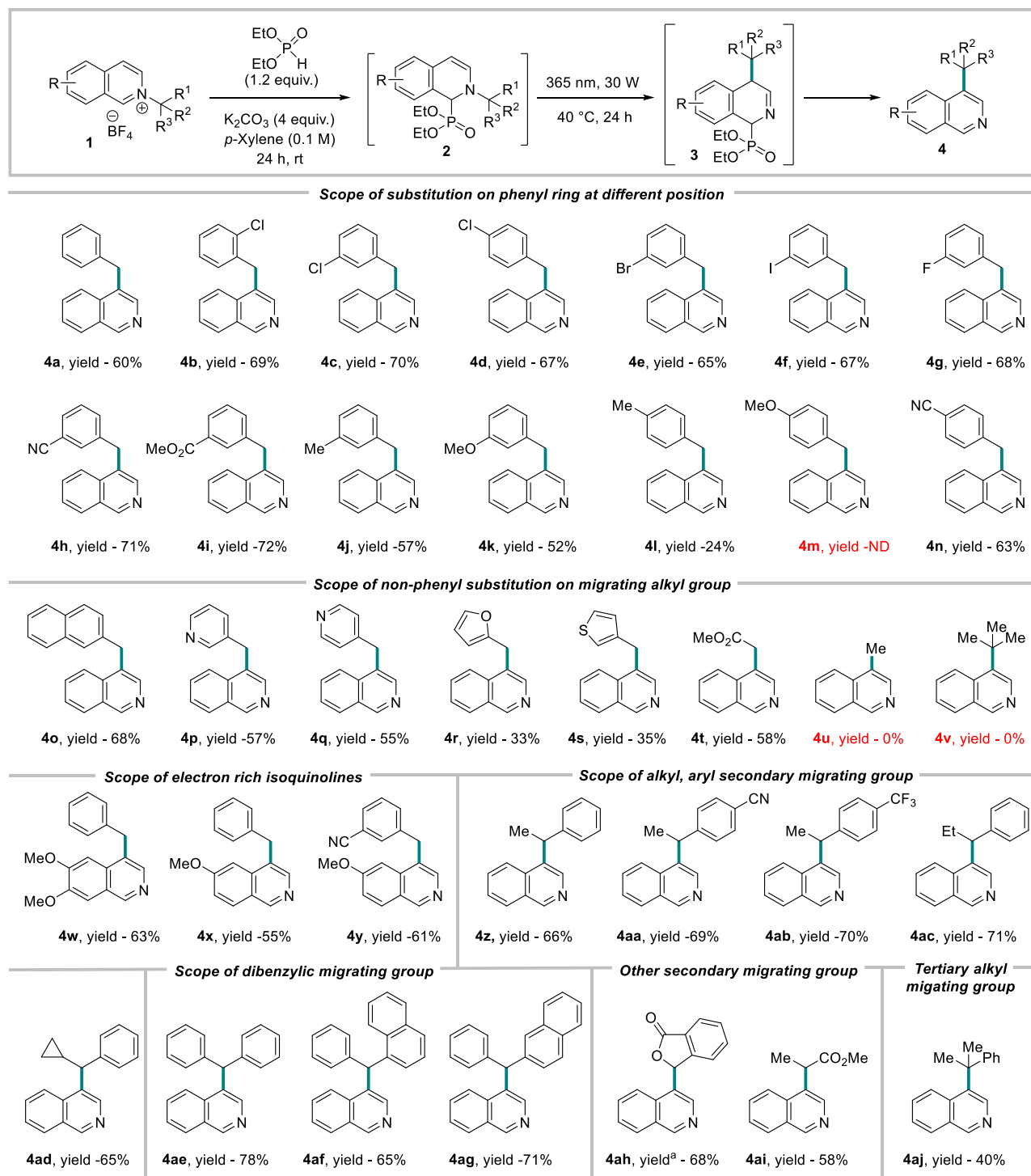


Figure 2. Substrate scope. All reactions were performed on 0.2 mmol scale. All yields are isolated. ^a1ah (0.2 mmol), Diethylphosphite (0.24 mmol), Et₃N (0.3 mmol) and 2.5 ml DCM, 24 h, -40 °C; K₂CO₃ (0.5 mmol), *p*-Xylene (0.1 M), 30W LED (λ_{\max} = 365 nm), 24 h, 15 °C.

fused benzene ring of the isoquinoline successfully yielded the corresponding products with similar efficiencies (**4w,x,y**).

Many of the bioactive isoquinolines with *meta*-alkyl substitution are tertiary alkyl groups.^{4,17} Therefore, we tested our method for the docking and migration of secondary alkyl halides. The more substituted tertiary alkyl docked starting materials (**1**) with alkyl and aryl substitution led to better yields than the parent benzyl group. A methyl and phenyl substitution on

the migrating carbon led to a 66% yield of the tertiary alkylated isoquinoline product (**4z**). Expectedly, a methyl and electron-poor aryl substitution resulted in slightly better yields (**4aa,ab**). An ethyl instead of methyl as the alkyl substitution is equally efficient (**4ac**). Interestingly, cyclopropyl as the alkyl substitution led to normal cyclopropyl product formation (**4ad**) without any detectable ring-opening product. The success of a wide variety of substituents on the migrating carbon makes this method

attractive as a general *meta*-C–H alkyl protocol. The better results with sterically demanding substituted alkyl groups complement the known *meta*-C–H alkylation methods where steric crowding led to poor yields or failed reactions.⁷ Migrations of dibenzylic groups were studied next, which led to the highest 78% yield for diphenyl substitution (**4ae**). Other diarylmethyl groups also worked well to form the triarylmethane products (**4af,ag**) in good yields. We also tested the docking and migration of an α -oxy aryl lactone (phthalide) substituted alkyl group due to their prevalence in natural products.¹⁸ Docking an alkyl group containing heteroatom is tricky due to its instability.¹⁹ A modified docking and photochemical transportation protocol with a milder triethylamine base at a lower temperature resulted in the successful migration of this sensitive group with 68% yield (**4ah**). A methyl and ester substituted alkyl also migrates successfully (**4ai**). Finally, we tested the migration of a tertiary alkyl group at the *meta*-C–H position. The dimethylphenyl substituted substrate successfully formed the product (**4aj**) with a 40% yield. Although the yield is lower, a quaternary carbon center formation at *meta*-C–H with an all carbon alkyl group has not been achieved previously. The increase in steric and nucleophilicity of tertiary alkyl group due to the extra methyl substitution might be the cause for moderate yield with substantial dimerization of migrating group.

Mechanistic Studies

Although photochemical *aza*-[1,3] migration is not known, various other photochemical [1,3] migrations are reported to undergo via a concerted pericyclic pathway²⁰ and dissociative mechanism with radical recombination²¹ or radical chain propagation.²² To understand our reaction path, we carefully analyzed our reactions to detect any intermediate and side-products formed in the reaction. In that effort, we found a 5–20% dimer (**5**) of the migrating alkyl group depending on their reactivity. Electron-rich benzyl radicals and tertiary alkyl radicals were more prone to dimerization. The degree of dimerization is inversely correlated to the yields of *meta*-alkylated product formation. This dimer formation suggests a homolytically dissociative mechanism for our *meta*-alkyl migration. We also isolated small amounts (5–10%) of *ortho*-phosphonate isoquinoline (**6**). We presume this might be formed via the single electron oxidation of the other radical partner (**R1**) (Figure 3A). The classical TEMPO trapping experiment led to the benzyl-TEMPO adduct (**7a**), further supporting homolytic C–N dissociation as the reaction initiation step (Figure 3B). A direct photochemical excitation of the adduct **2** excites it to the singlet state, and therefore, the C–N bond dissociation from either a singlet or triplet state is feasible. To experimentally distinguish between these two possibilities, we set to attain singlet and triplet excited states selectively to study their reactivity. A triplet quencher like naphthalene diminish the product formation by only 7%.²³ However, iridium based triplet photosensitizer with higher triplet energy than the adduct **2** (calculated to be 53.6 kcal/mol) led to 10% product formation under 450 nm light irradiation (Figure 3C).²⁴ No reaction occurred with direct 450 nm light excitation without iridium photosensitizer. These results indicate a major reaction path from singlet excited state with a minor triplet state component.

To shed light on the reaction mechanism, we conducted TDDFT and DFT computations with model dimethylphosphite adduct **2a** bearing a benzyl as the migrating group. We truncated the ethyl groups present on the phosphite to methyl groups

in order to reduce the computational cost. The first singlet excited state (S_1) was found to be the bright state, and the S_1 optimized intermediate $2s^*$ lies at 77.7 kcal/mol above the adduct **2a** (Figure 3E). The activation total energy (ΔE_0^\ddagger) for the C–N bond dissociation at S_1 surface was estimated to be +5.7 kcal/mol above the Franck-Condon geometry on the S_1 surface. The ΔE_0^\ddagger from S_1 equilibrium was found to be +14.8 kcal/mol. Alternatively, $2s^*$ could undergo inter-system crossing (ISC) to its triplet state T_1 forming intermediate $2t^*$. To check whether ISC is feasible, we computed the spin orbit coupling matrix elements (SOCME) at the CASSCF level including 3 singlets and 2 triplets at S_0 , S_1 and T_1 geometries (see SI for details). Since, all the spin orbit coupling matrix elements have paucity values ($< 1 \text{ cm}^{-1}$) the rate for ISC is expected to be significantly slow, making the dissociation at S_1 surface as the favored pathway.²⁵ This observation is expected according to El-sayed's rule²⁶ as the photoexcitations involved in **2a** are of only π - π^* nature (see SI). In order to obtain further insights into the photoexcited bond dissociation process, we performed relaxed potential energy scans considering the singlet ground state (S_0) and two most important excited states, namely, first excited singlet (S_1) and triplet states (T_1) using DFT/TDDFT (M062X/6-31++G(d,p)) (See SI for details). The density functional studies rather suggested a substantial barrier to dissociation on the S_1 surface.

Since, the chemical transformation involves a bond breaking scenario under photoexcitation, for obtaining more reliable estimates on energetics proper treatment of static and dynamic electron correlation is needed.²⁷ Hence, we carried out single point calculations on relevant DFT optimized geometries with strongly contracted n-electron valence state perturbation theory (SC-NEVPT2)²⁸ (see SI). According to the computed NEVPT2 energetics the barriers associated with the desired C–N bond cleavage are similar on both S_1 and T_1 surfaces. The NEVPT2 studies revealed that the TS lies just 4.6 kcal/mol above the Franck-Condon region on S_1 excited state surface (see SI). Hence, it can be expected that a significant fraction of photoexcited molecules will undergo C–N bond dissociation, while a larger fraction will relax to the S_1 minimum leading to fluorescence (which we experimentally observe). Furthermore, we theoretically studied the congener of **2a** having *p*-CN substitution at migrating phenyl group (**4n**, see SI) that gives higher experimental product yield. It was found that the TS for C–N photo-dissociation lies below the Franck-Condon geometry on the S_1 surface and only 2.6 kcal/mol above the S_1 minimum. Based on these observations and low computed SOCME values we propose this channel at S_1 to be the dominant pathway for C–N photo-dissociation.

Next, we tried to understand the C–C bond formation mechanism from the *bis*-radical intermediacy (**R1** & **R2**). Most photochemical [1,3] rearrangements were proposed to form C–X bonds via a radical-chain propagation mechanism.²² However, photoexcited aryl enamines with bicyclic N–O substituted compounds are reported to undergo [1,3] shift via intramolecular radical recombination.²¹ For our [1,3] alkyl shift, either the benzyl-benzyl (**R1** & **R2**) radical recombination to intermediate **3**, or a benzyl radical (**R2**) addition to the electron-rich enamine (**2**) for chain propagation could be kinetically challenging (Figure 3D). Both mechanistic pathways explain poor yields with electron-rich migrating alkyl radicals while better results with electron-deficient ones. We performed a crossover experiment with **1h** and **1x** to gain experimental evidence. The recombination mechanism should predominantly produce only normal

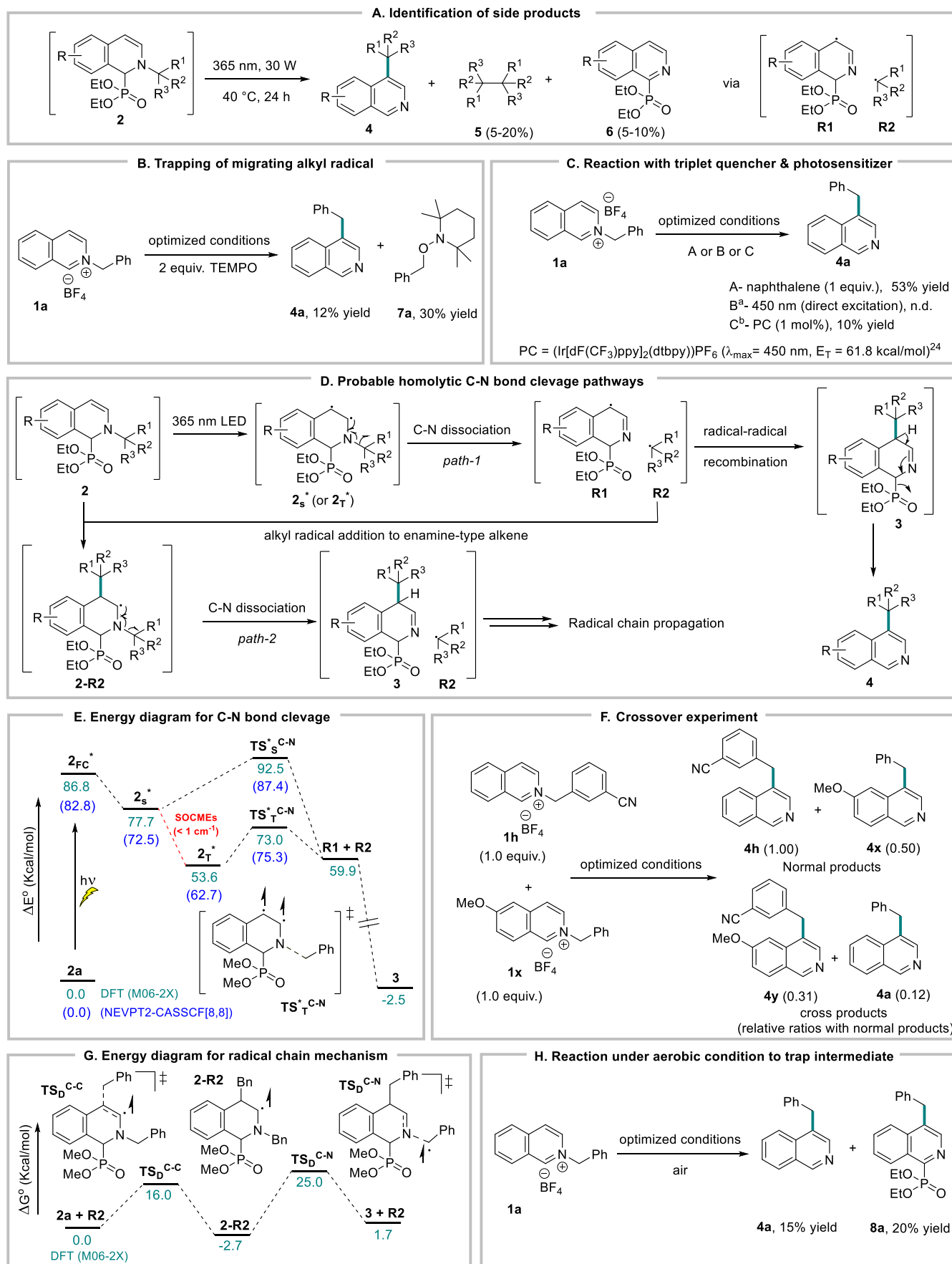


Figure 3. Mechanistic investigation. All reactions were performed on 0.2 mmol scale. Isolated yields are given. ^aMore than 95% intermediate remaining. ^b15% intermediate remaining. n.d. – not detected.

products (**4h** and **4x**), provided the concentration of the radicals is low at any point. On the other hand, the chain mechanism would generate all four products, including **4a** and **4y** (Figure 3F).²² The fact that we obtained major normal products with significant cross-products indicates the possibility of both pathways operating at variable degrees. The radical trapping experiment with TEMPO (Scheme 2B) did not completely shut down the product formation, which also suggests partial radical recombination via solvent-trapped intermediates (**R1** & **R2**).^{29,15b} The feasibility of radical chain propagation path was calculated next. The electrophilic migrating radical **R2** generated via C–N bond dissociation can attack another electron-rich adduct **2a** at the *meta*-position to form intermediate **2-R2**. The activation barrier for such addition is 16.0 kcal/mol with benzyl radical. Subsequent N–benzyl bond dissociation would form the *aza*-[1,3] migrated product (**3**) with another benzyl radical (**R2**) for chain propagation (Figure 3G). The activation barrier for the C–N bond dissociation from **2-R2** was calculated to be 27.7 kcal/mol, making it feasible at reaction temperature of 40 °C. Similar to the bond dissociation from **2**, the energy requirement from **2-R2** is also expected to be substrate dependent.

The final *meta*-alkylation product formation from the *aza*-[1,3] alkyl shifted intermediate **3** is proposed to undergo via a base-mediated 1,4-phosphite elimination. We exposed adduct **2a** to 365 nm light without any base to trap intermediate **3a**, but it resulted in very little product formation with no detectable intermediate. Quenching the reaction at different times and the analysis of the crude reaction mixture also failed to detect intermediate **3a** via mass or NMR. However, we could isolate around 9-13% of **8a**, which might form via aerobic oxidative aromatization of the dihydroisoquinoline intermediate **3a**. To validate this hypothesis, we ran the reaction in presence of air,

and that lead to a higher amount of **8a** formation (20%) along with **4a** (Figure 3H).

Phosphite mediated sequential docking and region-selective C–H functionalization. Sequential and regioselective C–H bond functionalization of isoquinolines is immensely attractive for the derivatization of the bioactive isoquinolines to improve and expand their potential drug candidacy. For example, *ortho*, *meta*-dialkyl isoquinolines are frequently screened for SAR studies in bioactivity assessment.³⁰ The synthesis of these regioselective double alkylated isoquinoline requires multiple steps with different alkylating reagents and catalysts. With our previous *ortho*-alkylation method from the same starting material **1** in hand,^{8b} we tested the feasibility of sequential docking and transfer of multiple alkyl groups regioselectively. In our first sequence, we docked *meta*-fluoro benzyl group (**1g**) for its photochemical transportation to *meta*-position of isoquinoline to **4g**. Subsequently, *meta*-chloro benzyl was docked on **4g** nitrogen to form the corresponding N-docked salt **9gc**. We treated **9gc** under our *ortho*-alkyl transportation method, successfully generating the *ortho*, *meta*-dialkylated product **10gc** with 45% yield. It is significant to note that benzyl docked on nitrogen can be selectively transported to either *ortho*- or *meta*-position via the same phosphite adduct **2**, only by varying basic vs photochemical reaction conditions. To further demonstrate the utility of this consecutive regioselective approach, we reverse the sequence of *meta*-fluoro and *meta*-chlorobenzyl docking. As a result, the regiodivergent dialkyl isoquinoline **10cg** formed successfully with complete selectivity. This unprecedented regiodivergency via a common phosphite adduct of N-alkyl docked isoquinoline gives us great control in functionalizing multiple C–H bonds to access densely functionalized isoquinolines (Figure 4A).

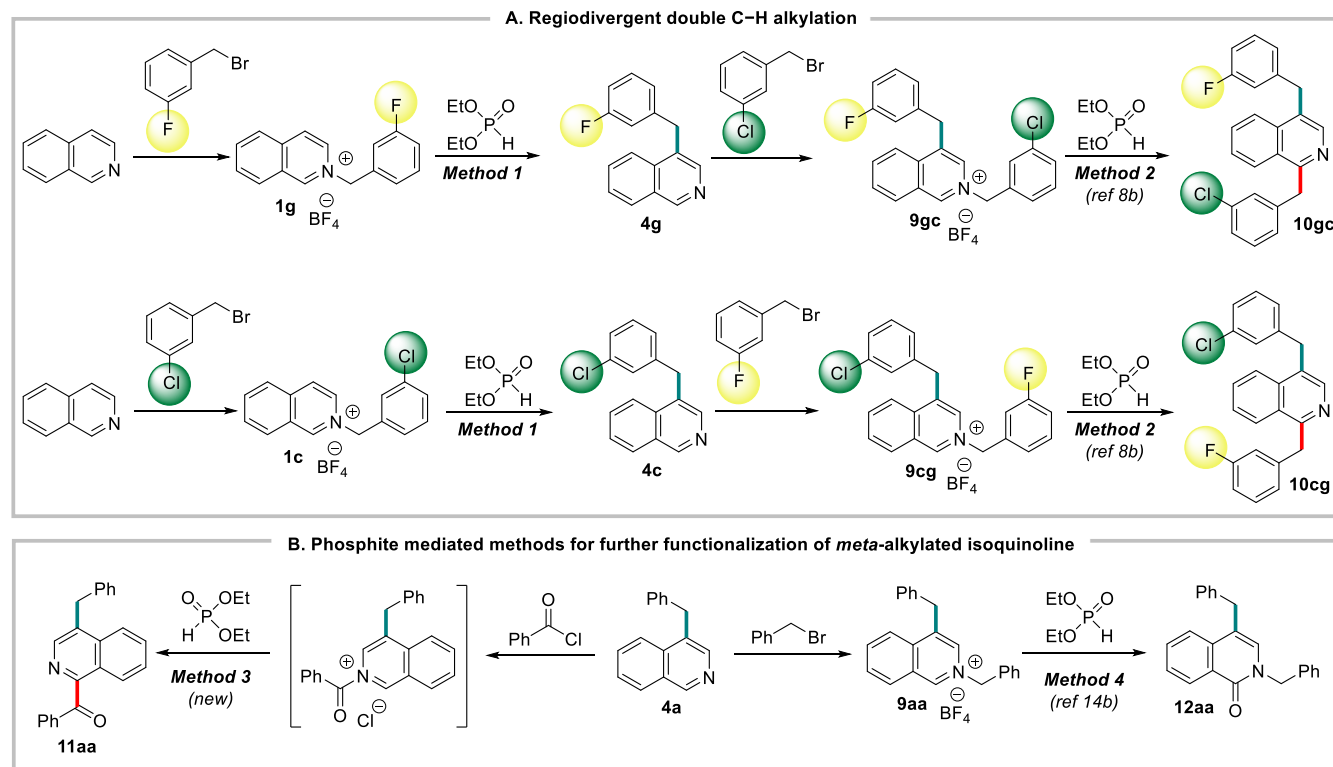


Figure 4. Phosphite mediated sequential docking and regio-selective multi-C–H functionalization of isoquinoline.

To further demonstrate the synthetic utility of the *meta*-alkylated product **4**, we attempted an unreported phosphite-mediated docking and *ortho*-transportation of an acyl (benzoyl) group.³¹ To our delight, the corresponding phosphite adduct underwent base mediated benzoyl migration to *ortho*-position smoothly to form *ortho*-acyl-*meta*-alkyl isoquinoline **11aa** with 68% yield. Next, we docked a second benzyl group on **4a**, and the docked intermediate was oxidized in air via another phosphite-mediated method to form *N*-benzylated isoquinoline **12aa** in good yield (Figure 4B).^{14b}

CONCLUSIONS

In summary, we have developed a new photochemical method for the transportation of a nitrogen-docked alkyl group on isoquinoline to its *meta*-position. This *meta*-C–H alkylation of isoquinoline works with all primary, secondary, and tertiary alkyl migrating groups to form sterically demanding secondary, tertiary, and an all carbon quaternary substitution. A variety of functional groups on

ASSOCIATED CONTENT

Supporting Information

The Supporting Information is available free of charge.

AUTHOR INFORMATION

Corresponding Author

Pradip Maity – Organic Chemistry Division, CSIR-National Chemical Laboratory, Pune-411008, India; orcid.org/0000-0001-8493-3171; Email: p.maity@ncl.res.in

Authors

Soniya Rani – Organic Chemistry Division, CSIR-National Chemical Laboratory, Pune-411008, India; Academy of Scientific and Innovative Research (AcSIR), Ghaziabad 201002, India; orcid.org/0000-0003-0929-3674

Anuj Kumar Ray – School of Chemical Sciences, Indian Association for the Cultivation of Science, Kolkata 700032, India; orcid.org/0000-0003-2034-6466

Devendra Kumar Dewangan – Organic Chemistry Division, CSIR-National Chemical Laboratory, Pune-411008, India; Academy of Scientific and Innovative Research (AcSIR), Ghaziabad 201002, India; orcid.org/0000-0002-4202-4989

Nita Aruna Ramchandra Patil – Organic Chemistry Division, CSIR-National Chemical Laboratory, Pune-411008, India; orcid.org/0009-0002-9224-2324

Aarthika M – Organic Chemistry Division, CSIR-National Chemical Laboratory, Pune-411008, India; Academy of Scientific and Innovative Research (AcSIR), Ghaziabad 201002, India; orcid.org/0009-0002-0197-1389

Ankan Paul – School of Chemical Sciences, Indian Association for the Cultivation of Science, Kolkata 700032, India; orcid.org/0000-0002-2380-8526; Email: rcap@iacs.res.in

Author Contributions

either migrating carbon or isoquinoline were tolerated. Sequential docking of alkyl groups on nitrogen, followed by phosphite-mediated method manipulations, led to double C–H alkylation to regiodivergent *ortho,meta*-dialkylation of isoquinoline. Other phosphite-mediated methods were also developed and utilized for further docking and functionalization of *meta*-C–H alkylated products. Both experimental and computational mechanistic studies were conducted to establish a probable reaction mechanism. Currently, we are studying the docking of other functional groups for their *meta*-migrations as a general waste-free strategy for *meta*-C–H functionalization of azaarenes.

The manuscript was written through the contributions of all authors. / All authors have approved the final version of the manuscript. / ‡S.R., A.K.R. and D.K.D. contributed equally.

Notes

The authors declare no competing financial interest.

ACKNOWLEDGMENT

This research was supported by the SERB (CRG/2019/001065 and SCP/2022/000465). S. R. and A. K. R. thank CSIR, D. K. D. and A. M thank INSPIRE for a fellowship. We thank Dr. Nilofar Baral for her experimental help. The support from the central analytical facility, NCL is greatly acknowledged.

REFERENCES

- (1) (a) Vitaku, E.; Smith, D. T.; Njardarson, J. T. Analysis of the Structural Diversity, Substitution Patterns, and Frequency of Nitrogen Heterocycles among U.S. FDA Approved Pharmaceuticals. *J. Med. Chem.* **2014**, *57*, 10257–10274. (b) Pal, S. Chapter 5, Pyridine, **2018**, ISBN 978-1-78923-423-7. <http://dx.doi.org/10.5772/intechopen.76986>. (c) Patil, P.; Sethy, S. P.; Sameera, T.; Shailaja, K. Pyridine and Its Biological Activity: A Review. *Asian J. Research Chem.*, **2013**, *6*, 888–899. (d) O'Hagan, D. Pyrrole, Pyrrolidine, Pyridine, Piperidine and Tropane Alkaloids. *Nat. Prod. Rep.*, **2000**, *17*, 435–446. (e) Shimizu, S.; Watanabe, N.; Kataoka, T.; Shoji, T.; Abe, N.; Morishita, S.; Ichimura, H. Pyridine and Pyridine Derivatives. Ullmann's Encyclopedia of Industrial Chemistry, Wiley-VCH: Weinheim, **2000**.
- (2) (a) Josephitis, C. M.; Nguyen, H. M. H.; McNally, A. Late-Stage C–H Functionalization of Azines. *Chem. Rev.* **2023**, *123*, 7655–7691. (b) Maity, S.; Bera, A.; Bhattacharjya, A.; Maity, P. C–H functionalization of pyridines. *Org. Biomol. Chem.* **2023**, *21*, 5671–5690. (c) Kerkovius, J. K.; Stegner, A.; Turlik, A.; Lam, P. H.; Houk, K. N.; Reisman, S. A Pyridine Dearomatization Approach to the Matrine-Type Lupin Alkaloids. *J. Am. Chem. Soc.* **2022**, *144*, 15938–15943.
- (3) (a) Bentley, K. W. β -Phenylethylamines and the Isoquinoline Alkaloids. *Nat. Prod. Rep.* **1992**, *9*, 365–391. (b) Chrzanowska, M.; Rozwadowska, M. D. Asymmetric Synthesis of Isoquinoline Alkaloids. *Chem. Rev.* **2004**, *104*, 3341–3370. (c) Chrzanowska, M.; Grajewska, A.; Rozwadowska, M. D. Asymmetric Synthesis of Isoquinoline Alkaloids: 2004–2015. *Chem. Rev.* **2016**, *116*, 12369–12465. (d) Kim, A. N.; Ngamthiporn, A.; Du, E.; Stoltz, B. M. Recent Advances in the Total Synthesis of the Tetrahydroisoquinoline Alkaloids (2002–2020). *Chem. Rev.* **2023**, *123*, 9447–9496.
- (4) (a) Zhang, Z.; Wang, J.; Li, J.; Yang, F.; Liu, G.; Tang, W.-J.; He, W.; Fu, J.-J.; Shen, Y.-H.; Li, A.; Zhang, W.-D.; Total Synthesis

- and Stereochemical Assignment of Delavatine A: Rh Catalyzed Asymmetric Hydrogenation of Indene-Type Tetrasubstituted Olefins and Kinetic Resolution through Pd Catalyzed Triflamide-Directed C–H Olefination. *J. Am. Chem. Soc.* **2017**, *139*, 5558–5567. (b) Palani, V.; Hugelshofer, C. L.; Kevlishvili, I.; Liu, P.; Sarpon, R. A Short Synthesis of Delavatine A Unveils New Insights into Site Selective Cross-Coupling of 3,5-Dibromo-2-pyrone. *J. Am. Chem. Soc.* **2019**, *141*, 2652–2660. (c) Hernandez, J. W.; Pospech, J.; Klöckner, U.; Bingham, T. W.; Sarlah, D.; Synthesis of (+)-Pancratistatin via Catalytic Desymmetrization of Benzene. *J. Am. Chem. Soc.* **2017**, *139*, 15656–15659. (d) Keck, G. E.; McHardy, S. F.; Murry, J. A. Total Synthesis of (+)-7-Deoxypancratistatin: A Radical Cyclization Approach. *J. Am. Chem. Soc.* **1995**, *117*, 7289–7290. (e) Yamada, K.; Yamashita, M.; Sumiyoshi, T.; Nishimura, K.; Tomioka, K. Total Synthesis of (–)-Lycorine and (–)-2-epi-Lycorine by Asymmetric Conjugate Addition Cascade. *Org. Lett.* **2009**, *11*, 1631–1633. (f) Beaulieu, M.-A.; Ottenwaelder, X.; Canesi, S. Asymmetric Synthesis of Fortucine and Reassignment of Its Absolute Configuration. *Chem. - Eur. J.* **2014**, *20*, 7581–7584. (g) McManus, H. A.; Fleming, M. J.; Lautens, M. Enantioselective Total Synthesis of (+)-Homochelidonine by a Pd II-Catalyzed Ring-Opening Reaction of a *meso*-Azabicyclic Alkene with an Aryl Boronic Acid. *Angew. Chem., Int. Ed.* **2007**, *46*, 433–436.
- (5) (a) Minisci, F.; Vismara, E.; Fontana, F.; Morini, G.; Serravalle, M.; Giordano, C. Polar Effects in Free-Radical Reactions. Rate Constants in Phenylation and New Methods of Selective Alkylation of Heteroaromatic Bases. *J. Org. Chem.*, **1986**, *51*, 4411–4416. (b) Lewis, J. C.; Bergman, R. G.; Ellman, J. A. Rh(I)-Catalyzed Alkylation of Quinolines and Pyridines via C–H Bond Activation. *J. Am. Chem. Soc.* **2007**, *129*, 5332–5333. (c) Andou, T.; Saga, Y.; Komai, H.; Matsunaga, S.; Kanai, M. Cobalt-Catalyzed C4-Selective Direct Alkylation of Pyridines. *Angew. Chem. Int. Ed.* **2013**, *52*, 3213–3216.
- (6) (a) Haley, H. M. S.; Payer, S. E.; Papidocha, S. M.; Clemens, S.; Nyehuis, J.; Sarpong, R. Bioinspired Diversification Approach Toward the Total Synthesis of Lycodine-Type Alkaloids. *J. Am. Chem. Soc.* **2021**, *143*, 4732–4740. (b) Laudadio, G.; Neigenfind, P.; Peter, A.; Rubel, C. Z.; Emmanuel, M. A.; Oderinde, M. S.; Ewing, T. E.-H.; Palkowitz, M. D.; Sloane, J. L.; Gillman, K. W.; Ridge, D.; Mandler, M. D.; Bolduc, P. N.; Nicastrì, M. C.; Zhang, B.; Clementson, S.; Petersen, N. N.; Martin-Gago, P.; Mykhailiuk, P.; Engle, K. M.; Baran, P. S. Nickel-Electrocatalytic Decarboxylative Arylation to Access Quaternary Centers. *Angew. Chem. Int. Ed.* **2024**, e202314617.
- (7) (a) Minter, D. E.; Re, M. A. A New Synthesis of 4-Substituted Isoquinolines. *J. Org. Chem.* **1988**, *53*, 2653–2655. (b) Liu, Z.; He, J.-H.; Zhang, M.; Shi, Z.-J.; Tang, H.; Zhou, X.-Y.; Tian, J.-J.; Wang, X.-C. Borane-Catalyzed C3-Alkylation of Pyridines with Imines, Aldehydes, or Ketones as Electrophiles. *J. Am. Chem. Soc.*, **2022**, *144*, 4810–4818. (c) Liu, Z.; Shi, Z.-J.; Liu, L.; Zhang, M.; Zhang, M.-C.; Gou, H.-Y.; Wang, X.-C. Asymmetric C3-Allylation of Pyridines. *J. Am. Chem. Soc.* **2023**, *145*, 11789–11797. (d) Tian, J.-J.; Li, R.-R.; Tian, G.-X.; Wang, X.-C. Enantioselective C3-Allylation of Pyridines via Tandem Borane and Palladium Catalysis. *Angew. Chem. Int. Ed.* **2023**, *62*, e202307697. (e) Muta, R.; Torigoe, T.; Kuninobu, Y. 3-Position-Selective C–H Trifluoromethylation of Pyridine Rings Based on Nucleophilic Activation. *Org. Lett.* **2022**, *24*, 8218–8222. (f) Cao, H.; Cheng, Q.; Studer, A. Radical and Ionic meta-C–H Functionalization of Pyridines, Quinolines, and Isoquinolines. *Science*. **2022**, *378*, 779–785. (g) Day, A. J.; Jenkins, T. C.; Kischkewitz, M.; Christensen, K. E.; Poole, D. L.; Donohoe, T. J. Metal and Activating Group Free C-4 Alkylation of Isoquinolines via a Temporary Dearomatization Strategy. *Org. Lett.* **2023**, *25*, 614–618.
- (8) (a) Motaleb, A.; Rani, S.; Das, T.; Gonnade, R. G.; Maity, P. Phosphite-Catalyzed C–H Allylation of Azaarenes via an Enantioselective [2,3]-Aza-Wittig Rearrangement. *Angew. Chem. Int. Ed.* **2019**, *58*, 14104–14109. (b) Rani, S.; Dash, S. R.; Bera, A.; Alam, M. N.; Vanka, K.; Maity, P. Phosphite Mediated Asymmetric N to C Migration for the Synthesis of Chiral Heterocycles from Primary Amines. *Chem. Sci.* **2021**, *12*, 8996–9003.
- (9) (a) Nakao, Y.; Yamada, Y.; Kashihara, N.; Hiyama, T. Selective C-4 alkylation of pyridine by nickel/Lewis acid catalysis. *J. Am. Chem. Soc.* **2010**, *132*, 13666–13668. (b) Jung, S.; Shin, S.; Park, S.; Hong, S. Visible-light-driven C4-selective alkylation of pyridinium derivatives with alkyl bromides. *J. Am. Chem. Soc.* **2020**, *142*, 11370–11375. (c) Lee, W.; Jung, S.; Kim, M.; Hong, S. Site-selective direct C–H pyridylation of unactivated alkanes by triplet excited anthraquinone. *J. Am. Chem. Soc.* **2021**, *143*, 3003–3012. (d) Choi, J.; Laudadio, G.; Godineau, E.; Baran, P. S. Practical and Regioselective Synthesis of C-4-Alkylated Pyridines. *J. Am. Chem. Soc.* **2021**, *143*, 11927–11933. (e) Jung, S.; Lee, H.; Moon, Y.; Jung, H.-Y.; Hong, S. Site-Selective C–H Acylation of Pyridinium Derivatives by Photoredox Catalysis. *ACS Catal.* **2019**, *9*, 9891–9896. (f) Gu, Y.; Shen, Y.; Zarate, C.; Martin, R. A mild and Direct Site selective sp² C–H Silylation of (Poly)Azines. *J. Am. Chem. Soc.* **2019**, *141*, 127–132. (g) Nishida, T.; Ida, H.; Kuninobu, Y.; Kanai, M. Regioselective Trifluoromethylation of N-Heteroaromatic Compounds using Trifluoromethyldifluoroborane Activator. *Nat. Commun.* **2014**, *5*, 3387–3392. (h) Jaric, M.; Haag, B. A.; Unsinn, A.; Karaghiosoff, K.; Knochel, P. Highly Selective Metalations of Pyridines and Related Heterocycles using new Frustrated Lewis Pairs or Tmp-zinc and Tmp-magnesium Bases with BF₃·OEt₂. *Angew. Chem., Int. Ed.* **2010**, *49*, 5451–5455.
- (10) (a) Rothbaum, J. O.; Motta, A.; Kratish, Y.; Tobin J. Marks, T. J. Chemodivergent Organolanthanide-Catalyzed C–H α -Mono-Borylation of Pyridines. *J. Am. Chem. Soc.* **2022**, *144*, 17086–17096. (b) Murphy, J. M.; Liao, X.; Hartwig, J. F. Meta Halogenation of 1,3-Disubstituted Arenes via Iridium-Catalyzed Arene Borylation. *J. Am. Chem. Soc.* **2007**, *129*, 15434–15435. (c) Yang, L.; Uemura, N.; Nakao, Y. meta-Selective C–H Borylation of Benzamides and Pyridines by an Iridium–Lewis Acid Bifunctional Catalyst. *J. Am. Chem. Soc.* **2019**, *141*, 7972–7979. (d) Yang, L.; Semba, K.; Nakao, Y. para-Selective C–H Borylation of (Hetero)Arenes by Cooperative Iridium/Aluminum Catalysis. *Angew. Chem. Int. Ed.* **2017**, *56*, 4853–4857. (e) Nakao, Y.; Kanyiva, K. S.; Hiyama, T. A Strategy for C–H Activation of Pyridines: Direct C-2 Selective Alkenylation of Pyridines by Nickel/Lewis Acid Catalysis. *J. Am. Chem. Soc.* **2008**, *130*, 2448–2449. (f) Zhang, T.; Luan, Y.-X.; Lam, N. Y. S.; Li, J.-F.; Li, Y.; Ye, M.; Yu, J.-Q. A Directive Ni Catalyst Overrides Conventional Site Selectivity in Pyridine C–H Alkenylation. *Nat. Chem.* **2021**, *13*, 1207–1213. (g) Tsai, C.-C.; Shih, W.-C.; Fang, C.-H.; Li, C.-Y.; Ong, T.-G.; Yap, G. P. A. Bimetallic Nickel Aluminum Mediated para-Selective Alkenylation of Pyridine: Direct Observation of η^2, η^1 -Pyridine Ni(0)-Al(III) Intermediates Prior to C–H Bond Activation. *J. Am. Chem. Soc.* **2010**, *132*, 11887–11889.
- (11) Sun, G.-Q.; Yu, P.; Zhang, W.; Zhang, W.; Wang, Y.; Liao, L.-L.; Zhang, Z.; Li, L.; Lu, Z.; Yu, D.-G.; Lin, S.; Electrochemical Reactor Dictates Site Selectivity in N-Heteroarene Carboxylations. *Nature*. **2023**, *615*, 67–72.
- (12) Cao, H.; Bhattacharya, D.; Cheng, Q.; Studer, A. C–H Functionalization of Pyridines via Oxazino Pyridine Intermediates: Switching to para-Selectivity under Acidic Conditions. *J. Am. Chem. Soc.* **2023**, *145*, 15581–15588.
- (13) Alwarsh, S.; Xu, Y.; Qian, S. Y.; McIntosh, M. C. Radical [1,3] Rearrangements of Breslow Intermediates. *Angew. Chem. Int. Ed.* **2016**, *55*, 355–358.
- (14) (a) Aggarwal, V. K.; Bae, I.; Lee, H.-Y.; Williams, D. T. Sulfur-Ylide-Mediated Synthesis of Functionalized and Trisubstituted Epoxides with High Enantioselectivity; Application to the Synthesis of CDP-840. *Angew. Chem., Int. Ed.*, **2003**, *42*, 3274–3278. (b) Motaleb, A.; Bera, A.; Maity, P. An Organocatalyst Bound α -Aminoalkyl Radical Intermediate for Controlled Aerobic Oxidation of Iminium Ions. *Org. Biomol. Chem.* **2018**, *16*, 5081–5085.
- (15) (a) Nasveschuk, C. G.; Rovis, T. The [1,3] O-to-C Rearrangement: Opportunities for Stereoselective Synthesis. *Org. Biomol. Chem.*, **2008**, *6*, 240–254. (b) Alam, M. N.; Dash, S. R.; Mukherjee, A.; Pandole, S.; Marelli, U. K.; Vanka, K.; Maity, P. [1,3]-Claisen Rearrangement via Removable Functional Group Mediated Radical Stabilization. *Org. Lett.* **2021**, *23*, 890–895.
- (16) Lown, J. W.; Akhtar, M. H.; McDaniel, R. S. Stereochemistry and Mechanism of the Thermal [1,3] Alkyl Shift of Stable 1,4-Dialkyl-1,4-dihydropyrazines. *J. Org. Chem.* **1974**, *39*, 1988–2006.
- (17) (a) Bhowmik, D.; Buzzetti, F.; Fiorillo, G.; Orzi, F.; Syeda, T. M.; Lombardi, P.; Kumar, G. S. Synthesis of new 13-diphenylalkyl Analogues of Berberine and Elucidation of their Base Pair Specificity and Energetics of DNA Binding. *Med. Chem. Commun.*, **2014**, *5*, 226–231.

- (b) Fan, T.; Cheng, Y.; Wei, W.; Zeng, Q.; Guo, X.; Guo, Z.; Li, Y.; Zhao, L.; Shi, Y.; Zhang, X.; Jiang, J.; Wang, Y.; Kong, W.; Song, D. Palmatine Derivatives as Potential Antiplatelet Aggregation Agents via Protein Kinase G/Vasodilator-Stimulated Phosphoprotein and Phosphatidylinositol 3-Kinase/Akt Phosphorylation. *J. Med. Chem.* **2022**, *65*, 7399–7413.
- (18) (a) Soriano, M. D. P. C.; Shankaraiah, N.; Santos, L. S. Short Synthesis of Noscapine, Bicuclline, Egenine, Capnoidine, and Corytensine Alkaloids through the Addition of 1-Siloxy-Isobenzofurans to Imines. *Tetrahedron Lett.* **2010**, *51*, 1770–1773. (b) Li, Y.; Smolke, C. D. Engineering Biosynthesis of the Anticancer Alkaloid Noscapine in Yeast. *Nat. Commun.* **2016**, *7*, 12137.
- (19) Zhu, J.; Bennet, A. J. Hydrolysis of (2-Deoxy- α -d-Glucopyranosyl)pyridinium Salts: The 2-Deoxyglucosyl Oxocarbenium Is Not Solvent-Equilibrated in Water. *J. Am. Chem. Soc.* **1998**, *120*, 3887–3893.
- (20) (a) Slutsky, J.; Kwart, H. Kinetics, Stereo-chemistry, and Mechanisms of the Silaallylic and Silapropynylic Rearrangements. *J. Am. Chem. Soc.* **1973**, *95*, 8678–8685. (b) Yamabe, T.; Nakamura, K.; Shitota, Y.; Yoshizawa, K.; Kawachi, S.; Ishikawa, M. Novel Aspects of the [1,3] Sigmatropic Silyl Shift in Allylsilane. *J. Am. Chem. Soc.* **1997**, *119*, 807–815. (c) Hammer, N.; Christensen, M. L.; Chen, Y.; Naharro, D.; Liu, F.; Jørgensen, K. A.; Houk, K. N. An Experimental Stereoselective Photochemical [1s,3s]-Sigmatropic Silyl Shift and the Existence of Silyl/Allyl Conical Intersections. *J. Am. Chem. Soc.* **2020**, *142*, 6030–6035.
- (21) (a) Wearing, E. R.; Blackmun, D. E.; Becker, M. R.; Schindler, C. S. 1- and 2-Azetines via Visible Light-Mediated [2 + 2]-Cycloadditions of Alkynes and Oximes. *J. Am. Chem. Soc.* **2021**, *143*, 16235–16242 (b) Gatazka, M. R.; McFee, E. C.; Ng, C. H.; Wearing, E. R. Schindler, C. S. New Strategies for the Synthesis of 1- and 2-Azetines and Their Applications as Value-Added Building Blocks. *Org. Biomol. Chem.* **2022**, *20*, 9052–9068.
- (22) (a) Su, X.; Huang, H.; Yuan, Y.; Li, Y. Radical Desulfur-Fragmentation and Reconstruction of Enol Triflates: Facile Access to a Trifluoromethyl Ketones. *Angew. Chem. Int. Ed.* **2017**, *56*, 1338–1341. (b) Xie, L.; Zhen, X.; Huang, S.; Su, X.; Lin, M.; Li, Y. Photoinduced Rearrangement of Vinyl Tosylates to β -ketosulfones. *Green Chem.*, **2017**, *19*, 3530–3534. (c) Wang, H.; Bellotti, P.; Zhang, X.; Paulisch, T. O.; Glorius, F. A Base-Controlled Switch of SO₂ Reincorporation in Photocatalyzed Radical Difunctionalization of Alkenes. *Chem.* **2021**, *7*, 3412–3424. (d) Silva, F. C. S.; Doktor, K.; Michaudel, Q. Modular Synthesis of Alkenyl Sulfamates and β -Ketosulfonamides via Sulfur(VI) Fluoride Exchange (SuFEx) Click Chemistry and Photomediated 1,3-Rearrangement. *Org. Lett.* **2021**, *23*, 5271–5276.
- (23) Giese, B.; Wettstein, P.; Stähelin, C.; Barbosa, F.; Neuburger, M.; Zehnder, M.; Wessig, P. Memory of Chirality in Photochemistry. *Angew. Chem. Int. Ed.* **1999**, *38*, 2586–2587.
- (24) Dutta, S.; Erchinger, J. E.; Strieth-Kalthoff, F.; Kleinmans, R.; Glorius, F. Energy Transfer Photocatalysis: Exciting Modes of Reactivity. *Chem. Soc. Rev.*, **2024**, *53*, 1068–1089.
- (25) Mavroskoufis, A.; Lohani, M.; Weber, M.; Hopkinson, M. N.; Gotze, J. P. A (TD-)DFT Study on Photo-NHC Catalysis: Photocyclization/Diels-Alder Reaction of Acid Fluorides Catalyzed by N-heterocyclic Carbenes. *Chem. Sci.* **2023**, *14*, 4027–4037.
- (26) Baba, M. Intersystem Crossing in the ¹n π * and ¹ $\pi\pi$ * States. *J. Phys. Chem. A* **2011**, *115*, 9514–9519.
- (27) Vijayasundar, J.; Subramanian, V.; Rajakumar, B. Excited State C-N Bond Dissociation and Cyclization of Tri-Aryl Amine-Based OLED Materials: A Theoretical Investigation. *Phys. Chem. Chem. Phys.* **2019**, *21*, 438–447.
- (28) Angeli, C.; Cimiraaglia, R.; Evangelisti, S.; Leininger, T.; Malrieu, J.-P.; Introduction of *n*-electron Valence States for Multireference Perturbation Theory. *J. Chem. Phys.* **2001**, *114*, 10252–10264.
- (29) (a) Bowry, V. W.; Luszyk, J.; Ingold, K. U. Calibration of a New Horology of Fast Radical “Clocks.” Ring-Opening Rates for Ring- and a-Alkyl-Substituted Cyclopropylcarbinyl Radicals and for the Bicyclo[2.1.0]pent-2-yl Radical. *J. Am. Chem. Soc.* **1991**, *113*, 5687–5698. (b) Martin-Esker, A. A.; Johnson, C. C.; Horner, J. H.; Newcomb, M. Picosecond Radical Kinetics. Fast Ring Openings of Constrained, Aryl-Substituted Cyclopropylcarbinyl Radicals. *J. Am. Chem. Soc.* **1994**, *116*, 9174–9181.
- (30) (a) Trost, B. M.; Hung, C.-I. J.; Jiao, Z. Enantioselective Divergent Syntheses of (+)-Bulleyanoline and Related Isoquinoline Alkaloids from the Genus *Corydalis*. *J. Am. Chem. Soc.* **2019**, *141*, 16085–16092. (b) Zhang, Q.; Tu, G.; Zhao, Y.; Cheng, T. Novel bioactive isoquinoline alkaloids from *Carduus crispus*. *Tetrahedron* **2002**, *58*, 6795–6798. (c) Gao, C.; Dua, Y.; Wanga, X.; Cao, H.; Lin, B.; Liua, Y.; Di, X. Hexahydrobenzophenanthridine Alkaloids from *Corydalis Bungeana Turcz.* and their Anti-inflammatory Activity. *Bioorg. Med. Chem. Lett.* **2018**, *28*, 2265–2269.
- (31) (a) Gibson, H. W.; Brumfield, K. K.; Gisle, R. A.; Hermann, C. K. F. Synthesis of Heterocyclic Monomers via Reissert Chemistry. *J. Polym. Sci.: Part A: Polym. Chem.* **2010**, *48*, 3856–3867. (b) Boekelheide, V.; Weinstock, J. Reissert Compounds. Further Alkylation Studies and a Novel Rearrangement. *J. Am. Chem. Soc.* **1952**, *74*, 660–663.